Journal Pre-proof

Dual-targeted alpha therapy mitigates prostate cancer and boosts immune checkpoint blockade therapy

Juan Sun, Jiangtao Yang, Jiakun Guo, Lei Tao, Bin Xu, Guanglin Wang, Fenghua Meng, Zhiyuan Zhong

PII: S0168-3659(25)00306-2

DOI: https://doi.org/10.1016/j.jconrel.2025.113686

Reference: COREL 113686

To appear in: *Journal of Controlled Release*

Received date: 1 February 2025

Revised date: 20 March 2025

Accepted date: 2 April 2025

Please cite this article as: J. Sun, J. Yang, J. Guo, et al., Dual-targeted alpha therapy mitigates prostate cancer and boosts immune checkpoint blockade therapy, *Journal of Controlled Release* (2024), https://doi.org/10.1016/j.jconrel.2025.113686

Dual-Targeted Alpha Therapy Mitigates Prostate Cancer and Boosts Immune Checkpoint Blockade Therapy

Juan Sun[1,2], Jiangtao Yang[1], Jiakun Guo[1], Lei Tao[1], Bin Xu[1], Guanglin Wang[3,*], Fenghua Meng[1], Zhiyuan Zhong[1,2,*]

[1] Biomedical Polymers Laboratory, College of Chemistry, Chemical Engineering and Materials Science, and State Key Laboratory of Radiation Medicine and Protection, Soochow University, Suzhou 215123, China

[2] College of Pharmaceutical Sciences, Soochow University, Suzhou 215123, China

[3] State Key Laboratory of Radiation Medicine and Protection, School of Radiation Medicine and Protection, Soochow University, Suzhou 215123, China

Corresponding Authors:

Guanglin Wang: glwang@suda.edu.cn

Zhiyuan Zhong: zyzhong@suda.edu.cn

Abstract

Alpha radionuclide with a high emitting energy and short emitting range has emerged as a new tool for the treatment of advanced tumors; however, its clinical usage stringently depends on delivery vehicle. Here, we report on Sigma-1 receptor and PSMA dual-specific peptide with efficient 225-actinium labeling (^{225}Ac-S1R/PSMA-P) for targeted alpha therapy and alpha-immunotherapy of murine prostate tumor. ^{225}Ac-S1R/PSMA-P with a high specific activity and radiostability exhibited upgraded cell binding and uptake while diminished efflux in RM1-PSMA^{+} cancer cells. Intriguingly, ^{225}Ac-S1R/PSMA-P afforded a peak uptake of 34.7 ± 3.2 %ID/g and elevated the radioactivity in the tumor over 7 days, with a tumor/kidney ratio of 12.2 ± 1.2 and minimal deposition in blood and other normal tissues like liver and muscle. A single injection of ^{225}Ac-S1R/PSMA-P effectively shrank large LNCaP-FGC tumors at 1.85 or 5.5 kBq, and completely eradicated highly malignant murine RM1-PSMA^{+}/RM1 tumors at 33.3 kBq. We further showed that ^{225}Ac-S1R/PSMA-P at a low dose of 3.7 kBq could boost immune checkpoint blockade therapy of murine RM1-PSMA^{+}/RM1 tumor, leading to 5 out of 7 mice tumor-free that showed durable antitumor immune memory. ^{225}Ac-S1R/PSMA-P with excellent targeting and immune activation ability has a great clinical potential for treating advanced prostate cancer patients.

Keywords

Nuclear medicine, prostate cancer, radionuclide therapy, immunotherapy, checkpoint blockade therapy.

1. Introduction

Nuclear medicine represents a rapidly advancing diagnosis and treatment modality for different diseases, particularly metastatic cancers[1-4]. Targeted radionuclide therapy (TRT) that delivers radionuclide to the diseased site offers a unique advantage of screening and treating patients as well as monitoring treatment effects using the same radioligand, elegantly achieving precision therapy[5-7]. Given their great clinical benefits, two TRT drugs, ^{177}Lu-DOTATATE and ^{177}Lu-PSMA-617, have been approved for the treatment of neuroendocrine tumors and metastatic castration-resistant prostate cancer (mCRPC), respectively [8, 9]. Of note, the accumulated clinical results show that only partial patients are responsive to current TRT with ^{177}Lu [10-12], which is associated with inadequate tumor accretion of radionuclide, modest energy of beta particles, and radiation resistance of tumor cells[13, 14]. We recently developed a Sigma-1 receptor and PSMA dual-specific peptide (S1R/PSMA-P) that labeled with ^{177}Lu achieved superior tumor uptake and retention and better TRT of LNCaP prostate tumor xenografts than ^{177}Lu-PSMA-617 control[15].

In contrast to beta particles, alpha particles possess a much higher linear energy transfer (LET) and a shorter tissue penetration range, which affords not only significantly more potent tumor killing effects but also largely reduced damage to healthy cells[16-18]. Many studies have confirmed that TRT with alpha particles is much more effective than that with beta particles in different tumor models[19-21]. Among the numerous alpha emitters, ^{225}Ac has attracted the most interest due to its favorable half-life ($t_{1/2}$ = 9.9 days), substantial net emission energy of 27 MeV per decay, and excellent coordination properties[22]. The preclinical and clinical studies have demonstrated the efficacy of ^{225}Ac-labeled radioligands in overcoming radiation resistance and improving tumor control[23-25]. It should be noted, however, that there is a very limited supply, in addition to a high cost, of alpha-emitting radionuclides like ^{225}Ac [26]. It is of critical importance for targeted alpha therapy (TAT) to

develop a highly efficient and stable delivery system, which uses as few ^{225}Ac as possible.

mCRPC is an immunologically cold tumor and current immunotherapy has demonstrated dismal clinical efficacy[27, 28]. The mCRPC patients treated with PD-1 immune-checkpoint blockade (ICB) showed an objective response rate of 3% - 5% in the Keynote-199 trial [29]. The alpha radiation was reported to induce immunogenic cell death (ICD) and yield an inflammatory phenotype, thereby sensitizing the tumor to immunotherapy[30]. The radiation-induced ICD would lead to the release of tumor-associated antigens and damage-associated molecular patterns (DAMPs)[31]. The administration of various alpha emitters, including ^{211}At, ^{224}Ra, ^{212}Pb, ^{225}Ac, and ^{223}Ra, has induced immune activation, with a subsequent enhancement in efficacy when combined with immune checkpoint inhibitors (ICIs)[32-35]. The combination of alpha-radionuclide therapy with immunotherapy may provide a novel treatment strategy for mCRPC patients.

Here, we report on dual-targeted alpha therapy based on radioligand S1R/PSMA-P and alpha-immunotherapy of malignant prostate tumor (**Scheme 1**). Remarkably, ^{225}Ac-S1R/PSMA-P at a one-third dose, exhibited superior antitumor efficacy to PSMA-single targeted counterpart in advanced prostate tumor models. ^{225}Ac-S1R/PSMA-P completely eradicated the malignant murine tumors at 33.3 kBq, and at a very low dose (3.7 kBq) synergized with ICB therapy, potentiating immunotherapy of “cold” prostate tumor. ^{225}Ac-S1R/PSMA-P with excellent targeting and immune activation abilities exhibits a high clinical potential for the treatment of advanced prostate cancer.

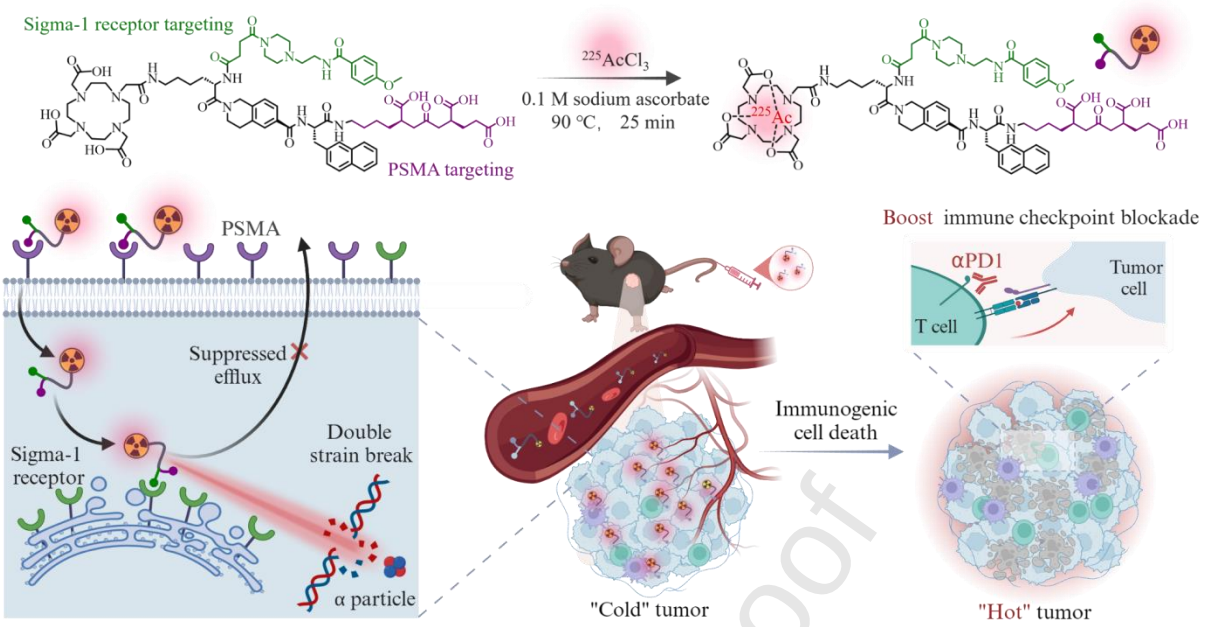

Scheme 1. Sigma-1 receptor and PSMA dual-specific radioligand (S1R/PSMA-P) for targeted alpha therapy and alpha-immunotherapy of murine prostate tumor. ^{225}Ac-S1R/PSMA-P achieves superior tumor accumulation and retention by binding to Sigma-1 receptor in the endoplasmic reticulum and minimizing drug efflux, leading to effective treatment of advanced human prostate tumor xenografts as well as malignant murine tumors. ^{225}Ac-S1R/PSMA-P at a very low dose (3.7 kBq) is capable of boosting immune checkpoint blockade therapy of "cold" murine prostate tumor.

2. Experimental

2.1 Materials

PSMA-617 was purchased from Topscience Co. Ltd. S1R/PSMA-P was kindly provided by Suzhou Ruihe Pharmaceutical Technology Co., Ltd. $^{225}Ac(NO_3)_3$ was purchased from the China Isotope & Radiation Corporation.

2.2 Radiosynthesis

The radiolabeling of S1R/PSMA-P followed the method previously described for ^{225}Ac-PSMA-I&T with slight modifications[36]. Briefly, 9.25 MBq of solid $^{225}Ac(NO_3)_3$ was

dissolved in 100 μL of 0.1 M HCl to obtain a $^{225}AcCl_3$ solution with a final concentration of 92.5 kBq/μL. 200 mg of S1R/PSMA-P was dissolved in 1 mL of 0.1 M sodium ascorbate and diluted to a final concentration of 3.7 μg/μL. Subsequently, 370 kBq of $^{225}Ac(NO_3)_3$ was mixed with 7.4 μg of S1R/PSMA-P followed by replenishing with 0.1 M sodium ascorbate to a total volume of 50 μL. The mixture was heated at 95 ℃ for 25 min and then diluted with 50 μL of 0.25 M sodium ascorbate buffer. The radiochemical yield (RCY) was determined by radio-TLC analysis. 37 kBq of mixture was spotted onto the bottom of TLC plate and 0.5 mL of sodium citrate (0.5 M, pH 5) was employed as a mobile phase. Once the solvent had reached the top, the strip was dried and left for 3 h and 24 h, respectively, to allow for the measurement of activity. The radiochemical yield was calculated based on the ratio of activity of ^{225}Ac-S1R/PSMA-P to the total radioactivity (Lablogic, Scan-RAM).

2.3 *In vitro* PSMA-binding assay

The RM1-PSMA$^+$ cells were obtained by transfecting RM1 cells with human PSMA and isolating monoclonal lines via flow cytometry [37]. The time-dependent binding and internalization of ^{225}Ac-S1R/PSMA-P were investigated in RM1-PSMA$^+$ and LNCaP-FGC cells at 5×10^4 cells/well in 24-well plates. The cells were incubated with 500 μL of ^{225}Ac-S1R/PSMA-P (185 Bq) or ^{225}Ac-PSMA-617 (185 Bq) for 1, 4, or 24 h, followed by washing, stripping of membrane-bound activity with glycine buffer (50 mM glycine and 100 mM NaCl, pH 3), and collection of internalized activity by NaOH (1 M) lysis. In the efflux study, cells were incubated with 500 μL of ^{225}Ac-S1R/PSMA-P (185 Bq) or ^{225}Ac-PSMA-617 (185 Bq) for 1 h under varying concentrations of haloperidol (0, 2, or 10 μM). Subsequently, the nonradioactive medium was replaced and incubated for a further 3 h. Binding in PSMA-negative PC3 and RM1 cells was assessed after a 4 h incubation. The radioactivity

was quantified using a gamma counter (PerkinElmer, Wallac 2480).

2.4 Biodistribution study in RM1-PSMA$^+$ tumor-bearing mice

All animal experiments were approved by the Animal Care and Use Committee of Soochow University and conducted according to the Guidelines for the Care and Use of Experimental Animals. C57BL/6 mice (5 - 6 weeks old, 20 - 22 g) were maintained under standard relative humidity (50 - 60%), temperature (22 ± 2°C), hygiene, and a 12 h light/dark cycle. The suspension of a mixture of RM1-PSMA$^+$ cells (4.5×10^6 cells) and RM1 cells (5×10^5 cells) was subcutaneously inoculated into the shoulder region of the mice in 100 μL of PBS and Matrigel (Corning, Arizona) at a 1:1 ratio. Once the tumors reached 100-200 mm^3, ^{225}Ac-S1R/PSMA-P (37 kBq) or ^{225}Ac-PSMA-617 (37 kBq) was administered intravenously (n = 3). Mice were sacrificed at 4, 24, 48, 96, and 168 h post-injection. Tumors and major organs including blood, heart, liver, spleen, lung, kidney, muscle, bone, and bladder were collected, weighed, and analyzed for radioactivity using a γ-counter. The gamma counting was postponed for 24 h to allow ^{225}Ac to reach the secular equilibrium state with its daughter radionuclides[38]. The activity of ^{225}Ac was detected within the energy window of 170 - 260 keV. The data were decay-corrected and expressed as a percentage of the injected dose per gram tissue (%ID/g).

$$A_{DC}=A_t\times e^{\frac{\ln(2)}{T_{1/2}}t} \quad (1)$$

$$\%ID/g=\frac{A_{DC}}{A_0\times m}\times 100 \quad (2)$$

Where A_{DC} is the decay-corrected radioactivity in the tissue at time t, A_t is the measured radioactivity in the tissue at time t, and A_0 is the total injected dose of radioactivity. $T_{1/2}$ represents the half-life of ^{225}Ac. The weight of the tissue (m) is expressed in grams and t is the time elapsed since the injection. The area under the curve (AUC) values were determined for

the radioactivity in the tumor, kidney, liver, muscle, and blood after the injection from 4 h to 168 h based on decay-corrected biodistribution data, using GraphPad Prism software. The tumor-to-normal tissue (T/N) ratio was calculated from the AUC values.

2.5 *In Vivo* Therapy

To investigate the therapeutic efficacy of ^{225}Ac-S1R/PSMA-P in PSMA-positive LNCaP-FGC tumor, the mice were intravenously injected with PBS, varying doses of ^{225}Ac-S1R/PSMA-P (1.85 kBq and 5.55 kBq), and 5.55 kBq of ^{225}Ac-PSMA-617 at an average tumor volume of 500 mm^3. Tumor volume and body weight were monitored twice a week. The toxicity of ^{225}Ac-S1R/PSMA-P was assessed in healthy mice with varying administration doses, ranging from 0 to 33.3 kBq. On the 27th day, the mice were sacrificed, and the blood samples were collected for routine blood analysis. For the mice treated with PBS or 33.3 kBq of ^{225}Ac-S1R/PSMA-P, blood samples were also collected for liver and kidney function tests. Major organs including heart, liver, spleen, lung, and kidney were collected, sliced, and analyzed using hematoxylin and eosin (H&E) staining.

The therapeutic efficacy of ^{225}Ac-S1R/PSMA-P in RM1-PSMA$^+$/RM1 tumor-bearing mice was studied by intravenously injecting PBS, varying doses of ^{225}Ac-S1R/PSMA-P (3.7 kBq, 11.1 kBq, and 33.3 kBq) or ^{225}Ac-PSMA-617 (11.1 kBq and 33.3 kBq) when the average tumor volume reached ca. 100 mm^3. Tumor volume and body weight were monitored twice a week. The tumor volume (mm^3) was calculated according to the following formula: $0.5 \times \text{length} \times \text{width}^2$. The survival rates of the mice were recorded. Mice were euthanized following ethical protocols when they exhibited signs of distress or rapid weight loss (20% from the initial weight). Furthermore, if the tumor size exceeded 2000 mm^3 or became necrotic or ulcerative, mice were also euthanized.

To assess whether ^{225}Ac-S1R/PSMA-P induce ICD in RM1-PSMA$^+$ cells, calreticulin

(CRT) surface exposure, a key ICD marker, was quantified. RM1-PSMA$^+$ cells were seeded at 1×10^5 cells/well in a 12-well plates, incubated overnight, and treated with PBS or ^{225}Ac-S1R/PSMA-P (3.7 kBq/mL, n = 3) for 48 h. Then, cells were stained with an anti-CRT antibody at 4 °C for 1 h, followed by incubation with an Alexa Fluor 647-conjugated secondary antibody at 4 °C for 30 min. CRT expression was analyzed via flow cytometry, and data were processed using FlowJo_V10.

To investigate the maturation of BMDCs stimulated by coculturing ^{225}Ac-S1R/PSMA-P and RM1-PSMA$^+$ cells, RM1-PSMA$^+$ cells were incubated with either PBS or ^{225}Ac-S1R/PSMA-P (3.7 kBq/mL, n = 3) for 48 h. BMDCs (1×10^6 /well) were then added and co-cultured for 24 h. BMDCs were collected, labeled with CD11c-FITC, CD80-APC, and CD86-PE/Cy7 antibodies at 4 °C for 30 min, and analyzed by flow cytometry.

To investigate the therapeutic efficacy of combination therapy of radiotherapy and immunotherapy, RM1-PSMA$^+$/RM1 tumor-bearing mice were randomly divided into four groups (n = 7): PBS, TAT (^{225}Ac-S1R/PSMA-P: 3.7 kBq), αPD1(10 μg), and TAT+αPD1 (^{225}Ac-S1R/PSMA-P: 3.7 kBq; αPD1: 10 μg). On day 0, ^{225}Ac-S1R/PSMA-P was intravenously administered and on days 1, 3, 5, and 7, αPD1 was intravenously administered. Tumor volume and body weight were measured twice a week post-injection. The survival rates of the mice were recorded. Mice were euthanized according to ethical protocols if they showed signs of distress or rapid weight loss (20% of initial weight) or tumor volume over 2000 mm^3.

To investigate the memory effect of combination therapy of radiotherapy and immunotherapy, five mice that had been cured were re-challenged with a suspension of the mixture of RM1-PSMA$^+$ cells (4.5×10^6 cells) and RM1 cells (5×10^5 cells) on day 120 after the first injection of ^{225}Ac-S1R/PSMA-P. Naïve mice inoculated with the mixture of RM1-PSMA$^+$ cells and RM1 cells were used as control. Tumor volume and body weight were

assessed twice a week. The date of death of the mice was recorded during the treatment. After 11 days, blood samples were collected, blocked with anti-mouse CD16/32, and stained with CD3-APC, CD8-PE/Cy7, CD44-FITC, and CD62L-PE. The cells were treated with RBC lysis/fixation solution for 10 min, washed and analyzed via flow cytometry to quantify $CD44^+CD62L^+$ central memory T cells (T_{CM}) and $CD44^+CD62L^-$ effector memory T cells (T_{EM}).

2.6 Immunological Analyses

To examine the immune responses associated with targeted alpha therapy combined with immunotherapy, RM1-$PSMA^+$ tumor-bearing mice were randomly divided into four groups (n = 4): PBS, TAT (^{225}Ac-S1R/PSMA-P: 3.7 kBq), αPD1(10 μg), and TAT+αPD1 (^{225}Ac-S1R/PSMA-P: 3.7 kBq; αPD1: 10 μg). On day 0, ^{225}Ac-S1R/PSMA-P was intravenously administered and on days 1, 3, and 7, αPD1 was intravenously administered. On day 8, peripheral blood, tumor, and spleen were harvested. Tumor and spleen were then ground into single cell suspensions. The cells were stained with Zombie-NIR, blocked with anti-mouse CD16/32, labeled with CD45.2-PerCP/Cy5.5, CD3-APC, CD8a-FITC and CD69-PE/Cy7, and analyzed using flow cytometry. Serum samples were obtained for the purpose of quantifying the concentrations of IFN-γ and TNF-α.

2.7 Statistical Analysis

All data in this manuscript are presented as mean ± SD. Statistical significance was calculated using two-tailed Student's t-test for two-group comparisons and one-way two-sided analysis of variance (ANOVA) for multiple comparisons. $p < 0.05$ was considered significant (*), < 0.01 (**) and < 0.001 (***) highly significant.

3. Results and Discussion

3.1 Radiosynthesis and cell-binding study of ^{225}Ac-S1R/PSMA-P

S1R/PSMA-P could be readily labeled with ^{225}Ac. The radiochemical yield of ^{225}Ac-S1R/PSMA-P exceeded 97%, as determined by radio-TLC (**Fig. 1a**). **Fig. 1b** illustrates that ^{225}Ac-S1R/PSMA-P displayed remarkable radiostability in PBS or serum at room temperature, with a radiochemical purity maintained over 90% in 7 days, warranting the subsequent *in vitro* and *in vivo* applications.

It has been demonstrated that the PSMA is highly expressed in over 90% of prostate cancer patients [39], while the Sigma-1 receptor is moderately expressed in 40% of such patients [40]. To investigate the combination of TAT and immune therapy, we have established a PMSA-positive murine cell line by transfecting RM1 cells with human PSMA. The expression of PSMA has been validated by flow cytometry (**Fig. S1**). RM1-PSMA$^+$ cells showed modest expression of Sigma-1 receptors on the membrane and abundant expression on endoplasmic reticulum (**Fig. S2**), which aligns with previous reports [41, 42]. ^{225}Ac-S1R/PSMA-P demonstrated superior binding toward RM1-PSMA$^+$ and LNCaP cells to PSMA-single targeted ^{225}Ac-PSMA-617, at different time points from 1 to 24 h (**Figs. 1c and S3**). **Fig. 1d** further shows that ^{225}Ac-S1R/PSMA-P was more efficiently internalized (over 2.0-fold) than ^{225}Ac-PSMA-617. The high internalization and low non-uptake dose of ^{225}Ac-S1R/PSMA-P (**Fig. S4**) means fewer ^{225}Ac and its daughters (^{221}Fr, ^{217}At, and ^{213}Bi) being directly exposed to the extracellular environment [43]. Interestingly, ^{225}Ac-S1R/PSMA-P demonstrated approximately 3.7-fold lower efflux in RM1-PSMA$^+$ compared to control (**Figs. 1e**). The addition of haloperidol, an antagonist to σ receptors, to the culture medium resulted in increased efflux of ^{225}Ac-S1R/PSMA-P in both RM1-PSMA$^+$ and LNCaP cells (**Figs. 1e and S5**), confirming enhanced tumor cell retention via binding to Sigma-1 receptors. In contrast, haloperidol had little influence on the single PSMA-targeted

control. In PSMA-negative RM1 and PC3 cells, ^{225}Ac-S1R/PSMA-P demonstrated minimal binding **(Fig. 1f)**. It is evident, therefore, that the selective cell binding and endocytosis of ^{225}Ac-S1R/PSMA-P in RM1-PSMA^{+} cells is mainly mediated by PSMA. Following internalization, ^{225}Ac-S1R/PSMA-P binds to the Sigma-1 receptor in the endoplasmic reticulum, which effectively enhances intracellular drug retention by inhibiting drug efflux. This extracellular and intracellular sequential targeting strategy of ^{225}Ac-S1R/PSMA-P is unique because it boosts drug accumulation/retention inside target cells but not in other cells.

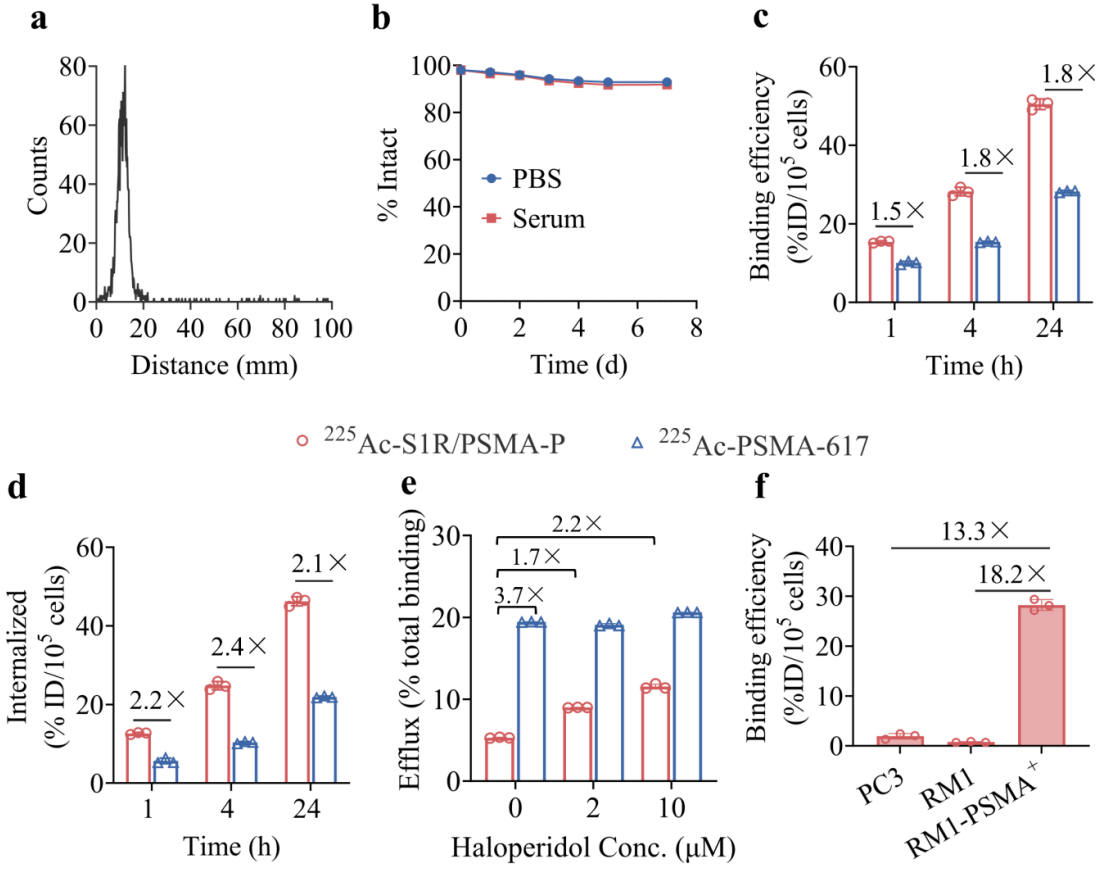

Fig. 1 Radiolabeling, *in vitro* stability and cellular uptake assessment of ^{225}Ac-S1R/PSMA-P. (a) Radiolabeling efficiency analyzed by radio-TLC. (b) The radiostability of ^{225}Ac-S1R/PSMA-P incubated with PBS or serum at room temperature over 7 days analyzed by radio-TLC. Binding efficiency (c) and internalization (d) of ^{225}Ac-S1R/PSMA-P and ^{225}Ac-PSMA-617 at incubation with RM1-PSMA^{+} cells for 1, 4, or 24 h. (e) Efflux of ^{225}Ac-S1R/PSMA-P and ^{225}Ac-PSMA-617 in RM1-PSMA^{+} cells after 3 h treatment with various concentrations of haloperidol (0, 2, or 10 μM). (f) Binding efficiency of

^{225}Ac-S1R/PSMA-P incubated in RM1-PSMA^{+}, PC3 or RM1 cells for 4 h (n = 3).

3.2 Biodistribution and Pharmacokinetics of ^{225}Ac-S1R/PSMA-P

The biodistribution of ^{225}Ac-S1R/PSMA-P was studied in murine RM1-PSMA^{+} tumor model, which was established by subcutaneously inoculating a mixture of RM1-PSMA^{+} cells (4.5 × 10^6 cells) and RM1 cells (5 × 10^5 cells). RM1-PSMA^{+}/RM1 tumor is a highly malignant model, reaching a volume of 1500 mm^3 within 14 days. **Fig. 2a** shows a great tumor uptake of ^{225}Ac-S1R/PSMA-P, reaching 34.7 ± 3.2 %ID/g at 4 h post-injection，which was approximately 2.0-fold that of ^{225}Ac-PSMA-617 (**Fig. 2b**). Interestingly, ^{225}Ac-S1R/PSMA-P demonstrated superior tumor retention, with tumor level remained 26.1 ± 1.2 %ID/g at 96 h post-injection and increased to 81 ± 1.2 %ID/g at 168 h due to notable reduction in tumor volume. Giving its half-life of 9.9 days, the alpha radioactivity in the tumor did not decrease but increased at prolonged time. Throughout the observation period (4 - 168 h), ^{225}Ac-S1R/PSMA-P demonstrated superior tumor accumulation, in which a 5.8-fold higher area under the curve (AUC) was observed for ^{225}Ac-S1R/PSMA-P over ^{225}Ac-PSMA-617 (**Fig. 2c**). In contrast to the high expression of PSMA in mouse kidneys, PSMA is moderately expressed in human kidneys. It is less likely that significant renal toxicity will occur in humans if no toxicity is observed in mice[44]. Furthermore, the low uptake of the liver corroborated the stable chelation, as free ^{225}Ac has a proclivity to distribute in this organ[45]. In comparison to ^{225}Ac-PSMA-617, ^{225}Ac-S1R/PSMA-P exhibited higher tumor-to-normal tissue (T/N) ratios, e.g. 2.1-fold, 1.4-fold, 3.2-fold and 3.9-fold higher T/N ratios in the kidney, liver, muscle, and bone, respectively (**Fig. 2d**). The elevated T/N ratios signified enhanced selectivity and a more favorable therapeutic index for ^{225}Ac-S1R/PSMA-P. **Fig. S6** shows a nearly linear decrease of ^{225}Ac in the tumor, which extrapolated a tumor elimination time of approximately 194 h. In addition to its high energy, ^{225}Ac-S1R/PSMA-P also exhibited

advantages of much higher tumor uptake and retention compared with ^{177}Lu-PSMA-617 control in RM1-PSMA^{+} model (results of ^{177}Lu-PSMA-617 shown in **Fig. S7**).

The pharmacokinetics of ^{225}Ac-S1R/PSMA-P were investigated in healthy male C57BL/6 mice. ^{225}Ac-S1R/PSMA-P exhibited rapid elimination from the bloodstream with a half-life of 0.16 h, which was comparable to that of ^{225}Ac-PSMA-617 (**Fig. 2e**) and ^{177}Lu-PSMA-617 [15]. This rapid blood clearance is beneficial because it can minimize the amount of daughter radionuclides of ^{225}Ac to blood due to the recoil effect and differing chemical properties of the daughter radionuclides[46], and it can effectively reduce off-target toxicity by minimizing exposure to non-target tissues.

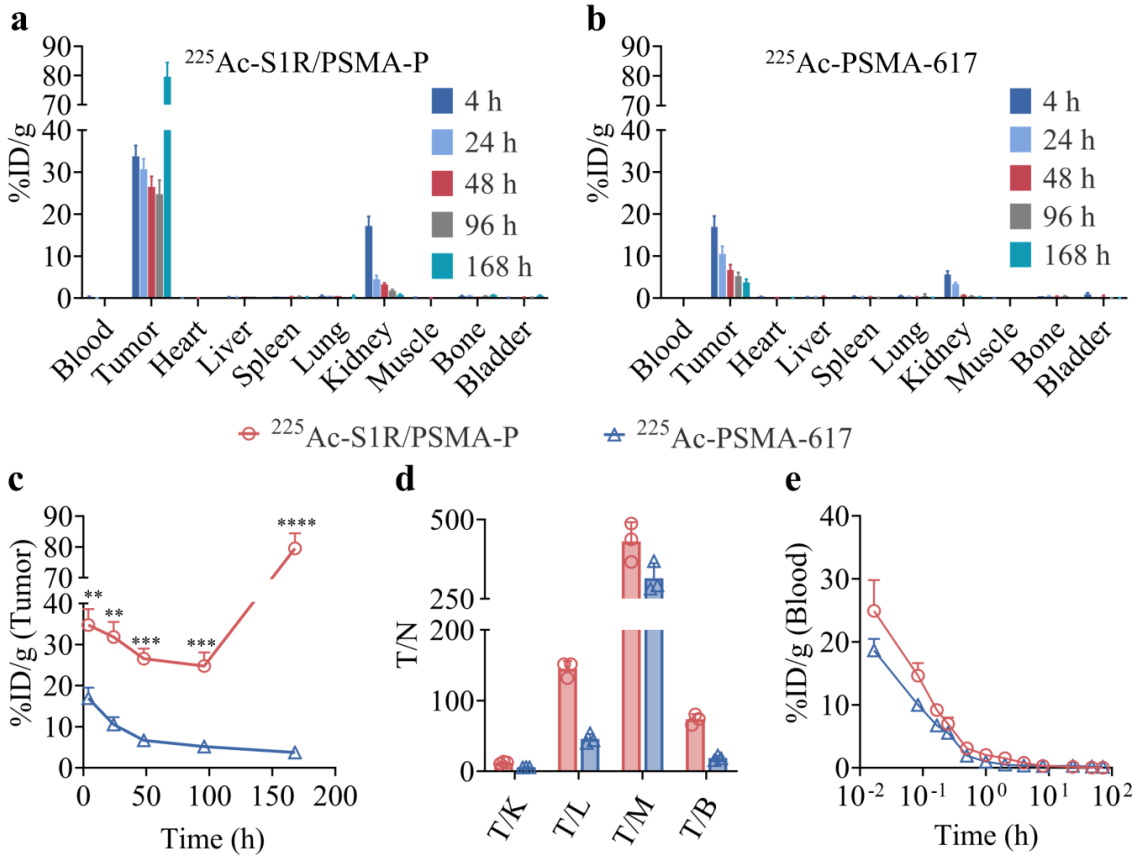

Fig. 2 The biodistribution of ^{225}Ac-S1R/PSMA-P (37 kBq) (a) and ^{225}Ac-PSMA-617 (37 kBq) (b) in RM1-PSMA^{+}/RM1 tumor-bearing mice at indicated time points post-injection (n = 3). (c) Accumulation of ^{225}Ac-S1R/PSMA-P and ^{225}Ac-PSMA-617 in tumor over time and their (d) tumor-to-normal tissue (T/N) ratio. T/K: tumor to kidney, T/L: tumor to liver, T/M: tumor to muscle, T/B: tumor to bone. (e) Pharmacokinetics of ^{225}Ac-S1R/PSMA-P and

^{225}Ac-PSMA-617 in healthy male C57BL/6 mice after intravenous injection (37 kBq) (n = 3). Statistical significance was analyzed by student t-test, ** $p < 0.01$, *** $p < 0.001$ and **** $p < 0.0001$.

3.3 Targeted Radionuclide Therapy of Prostate Tumor

The *in vivo* antitumor efficacy of ^{225}Ac-S1R/PSMA-P was evaluated in PSMA-positive LNCaP-FGC and RM1-PSMA^{+}/RM1 tumor models. The LNCaP-FGC tumor-bearing NCG mice, which are deficient in functional/mature T, NK and B cells, were randomly divided into four groups (n = 5) and intravenously injected with PBS, ^{225}Ac-S1R/PSMA-P (1.85 kBq or 5.55 kBq), and ^{225}Ac-PSMA-617 (5.55 kBq), respectively (**Fig. 3a**). LNCaP-FGC tumor is highly malignant, and the treatment was started when tumor volume reached approximately 500 mm^3 (advanced tumor model). **Fig. 3b** shows that ^{225}Ac-S1R/PSMA-P effectively shrank tumor even at a low dose of 1.85 kBq, while progressive tumor growth was observed for ^{225}Ac-PSMA-617 at 5.55 kBq. In light of the global scarcity and high cost of ^{225}Ac, reducing the alpha dosage will not only ensure better patient safety but also greatly reduce financial burdens, thereby enhancing the accessibility of therapy[47]. There was no significant loss of body weight of the mice during all treatments (**Fig. 3c**). The above results corroborate that ^{225}Ac-S1R/PSMA-P induces potent inhibitory effect for advanced prostate cancer.

The safety of ^{225}Ac-S1R/PSMA-P was assessed in healthy BALB/c mice (n = 5). The results showed that a single injection of ^{225}Ac-S1R/PSMA-P at 3.7 kBq, 11.1 kBq, or 33.3 kBq did not cause significant changes in body weight over the 27-day observation period (**Fig. 3d**). The routine blood analysis of mice treated with ^{225}Ac-S1R/PSMA-P at 3.7 kBq to 33.3 kBq, showed comparable levels of white blood cells, red blood cells, and platelets to those observed in healthy mice (**Figs. 3e, 3f, and 3g**). Liver and kidney function tests of mice treated with 33.3 kBq of ^{225}Ac-S1R/PSMA-P showed no significant differences compared to

healthy mice (**Fig. S8**). No discernible abnormalities in the main organs of mice were observed even at the highest dose of 33.3 kBq (**Fig. 3h**). The above results collectively indicate that ^{225}Ac-S1R/PSMA-P is well tolerated.

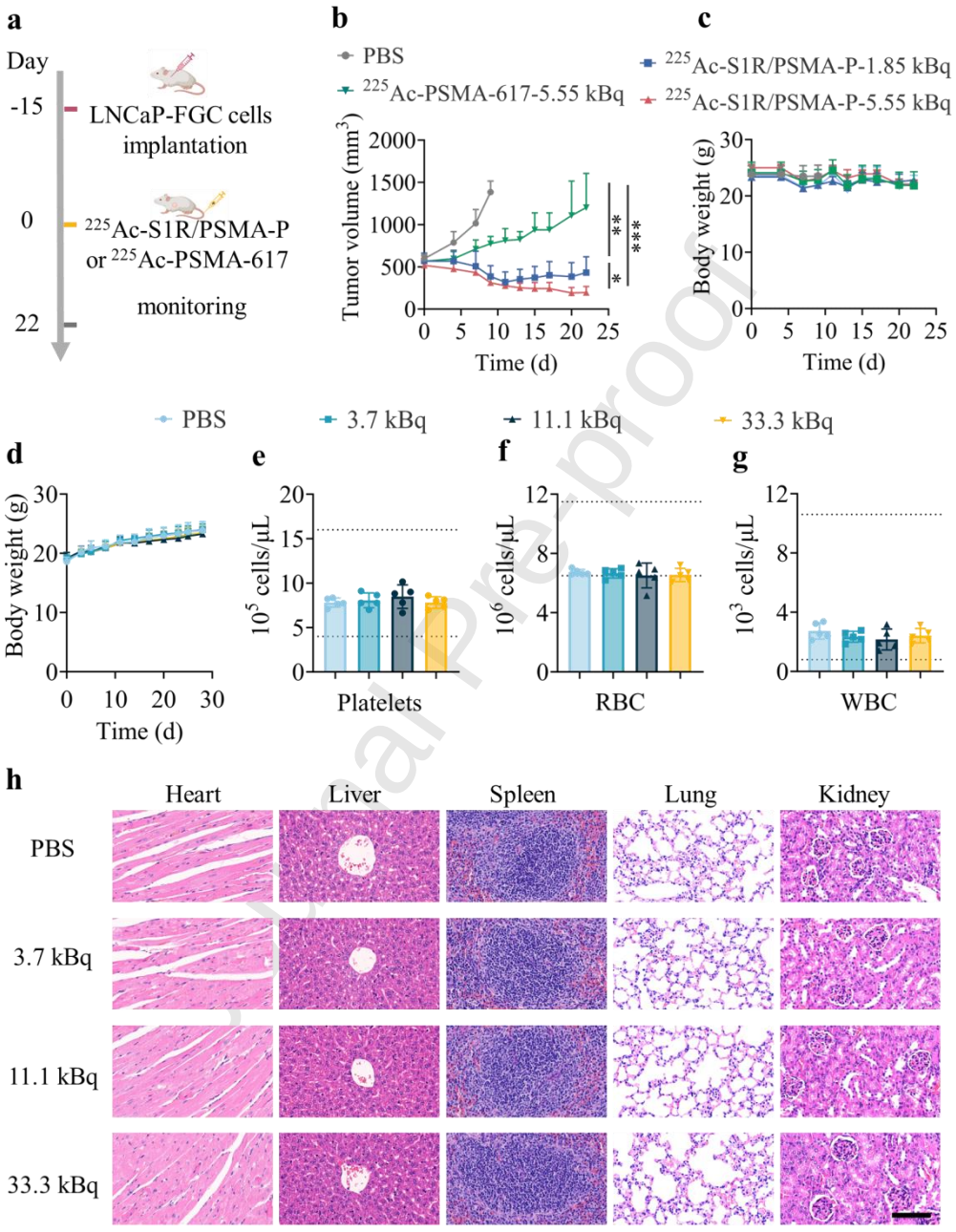

Fig. 3 Therapeutic activity of ^{225}Ac-S1R/PSMA-P at various doses in advanced LNCaP-FGC tumor-bearing NCG mice (a - c) and toxicity of ^{225}Ac-S1R/PSMA-P in healthy C57BL/6 mice (d - h). (a) Experimental schedule for figures b and c. (b) Tumor growth curves and (c) average body weight of the mice (n = 5) using ^{225}Ac-PSMA-617 as control. (d) Body weight changes of mice after intravenous injection of ^{225}Ac-S1R/PSMA-P at varying doses from 3.7

to 33.3 kBq, and (e - g) analysis of blood cells and (h) H&E stained images of major organs of healthy mice on day 27 post intravenous injection. Scale bar corresponds to 100 μm. WBC: white blood cells, RBC: red blood cells, PLT: platelets. Statistical significance was analyzed by student t-test, * $p < 0.1$, ** $p < 0.01$, and *** $p < 0.001$.

The efficacy of ^{225}Ac-S1R/PSMA-P was further investigated in RM1-PSMA^{+}/RM1 tumor-bearing mice when tumor volume reached approximately 150 mm^3. The mice were randomly divided into four groups (n = 5) and intravenously injected with PBS, ^{225}Ac-S1R/PSMA-P at three different doses (3.7, 11.1, or 33.3 kBq), and ^{225}Ac-PSMA-617 at two different doses (11.1 or 33.3 kBq), respectively (**Figs. 4a**). Intriguingly, a single dose of ^{225}Ac-S1R/PSMA-P at 3.7 kBq, 11.1 kBq, and 33.3 kBq resulted in 20%, 40%, and 100% complete regression (CR), respectively (**Figs. 4b, 4c**). In comparison, ^{225}Ac-PSMA-617 at 11.1 and 33.3 kBq only achieved 20% and 40% complete response (CR). It is of interest to note that ^{225}Ac-S1R/PSMA-P at 11.1 kBq greatly prolonged median survival time, reaching 67 days, which surpassed that for ^{225}Ac-PSMA-617 at 11.1 kBq (27 days) and 33.3 kBq (37 days). There was no significant body weight loss during the treatments (**Fig. 4d**). The above results confirm that ^{225}Ac-S1R/PSMA-P is far more effective than PSMA single targeted control, and is capable of eradicating malignant murine prostate cancer.

Alpha radiation has the capacity to modulate the tumor microenvironment by inducing ICD of tumor cells and further stimulating antigen-presenting cells[48-50]. We evaluated the ICD induction of ^{225}Ac-S1R/PSMA-P at 3.7 kBq/mL by detecting the production of calreticulin (CRT), a typical marker of ICD. The results revealed that ^{225}Ac-S1R/PSMA-P induced a substantial elevation in CRT (**Figs. 4e and 4f**). It has been demonstrated that ^{213}Bi, ^{223}Ra, and ^{211}At induce the pro-inflammatory damage-associated molecular patterns, including CRT, HMGB1, and HSP70, which are hallmarks of tumor immunogenicity[51-53]. The studies on stimulation of dendritic cells (DCs) co-cultured with RM1-PSMA^{+} cells by

^{225}Ac-S1R/PSMA-P demonstrated significantly stimulated maturation of BMDCs ($CD11c^+CD80^+CD86^+$, mDCs) by up to 13.6% (**Figs. 4g and 4h**), which is in line with previous reports that alpha radiation could elicit DCs maturation and boost cancer immunity[32, 34]. Hence, the therapeutic effect of ^{225}Ac-S1R/PSMA-P most likely derives from not only direct damaging of tumor cells via alpha particles but also activating the immune cells.

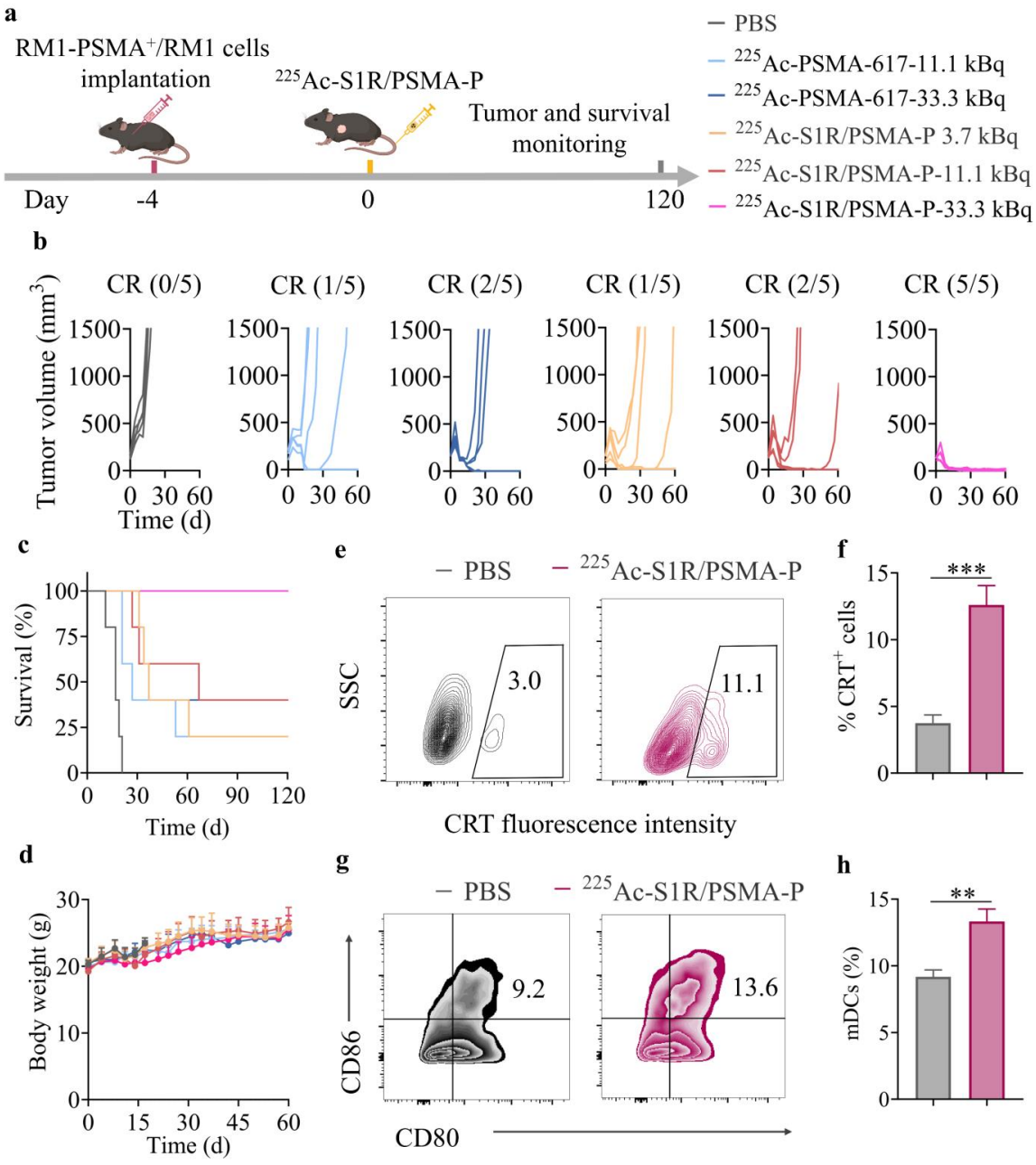

Fig. 4 Therapeutic activity of ^{225}Ac-S1R/PSMA-P at various doses in RM1-PSMA$^+$/RM1 tumor-bearing mice. (a) Experimental schedule. (b) Individual tumor growth curves, (c)

Kaplan-Meier survival curves, and (d) average body weight of mice treated with ^{225}Ac-S1R/PSMA-P (3.7, 11.1, or 33.3 kBq) or ^{225}Ac-PSMA-617 (11.1 or 33.3 kBq) (n = 5). (e) Representative flow cytometry graphs and (f) percentage of CRT of RM1-PSMA$^+$ cells treated with ^{225}Ac-S1R/PSMA-P (3.7 kBq/mL) for 48 h. (g) Representative flow cytometry graphs and (h) percentage of mature BMDCs (CD11c$^+$CD80$^+$CD86$^+$, mDCs) stimulated by ^{225}Ac-S1R/PSMA-P (3.7 kBq/mL). Statistical significance was analyzed by student t-test, ** $p < 0.01$ and *** $p < 0.001$.

3.4 ^{225}Ac-S1R/PSMA-P boosts immune checkpoint blockade therapy

The alpha therapy has shown capable of improving the immune responses of "cold" tumors like prostate tumor to a certain extent[54, 55]. Here, we studied whether a low dose (3.7 kBq) of ^{225}Ac-S1R/PSMA-P could boost PD-1 therapy (**Fig. 5a**). As expected, αPD-1 monotherapy failed to achieve any tumor control. The combination of ^{225}Ac-S1R/PSMA-P and αPD-1, however, effectively inhibited tumor growth and 5/7 mice achieved CR over 120 days (**Figs. 5b**, **5c**, and **5d**). Importantly, the combo group did not cause body weight loss (**Fig. 5e**). These treatment results are remarkable compared with previous report with ^{225}Ac-PSMA-617 and αPD-1, in which 2/8 mice achieved CR at 30 kBq[54]. This may be due to the much better tumor enrichment and retention of ^{225}Ac-S1R/PSMA-P compared to ^{225}Ac-PSMA-617, potentially activating a more sustained immune response[56].

To further evaluate the immune memory generated by the combination therapy, we re-challenged the cured mice with a mixture of RM1-PSMA$^+$ and RM1 cells on day 120 after the initial alpha therapy. Healthy mice inoculated with a mixture of RM1-PSMA$^+$ and RM1 cells was served as a control. In contrast to rapid tumor growth in the control group, tumor growth was significantly retarded in the cured mice (**Figs. 5f and 5g**). Notably, 3/5 mice showed full protection from the re-challenge, suggesting ^{225}Ac-S1R/PSMA-P in combination with αPD-1 induces strong and long-lasting immunity. The blood analysis showed that the percentage of CD8$^+$ effector memory T cells (T_{EM}, CD44$^+$CD62L$^-$) in CD8$^+$ T cells increased

from 14% for the control to 29% (**Figs. 5h and 5i**), suggesting a strong immune memory against tumor cells. The finding that a low dose of ^{225}Ac-S1R/PSMA-P can effectively boost the immune checkpoint blockade therapy of prostate tumor is remarkable, as it may provide a new treatment perspective for prostate cancer patients.

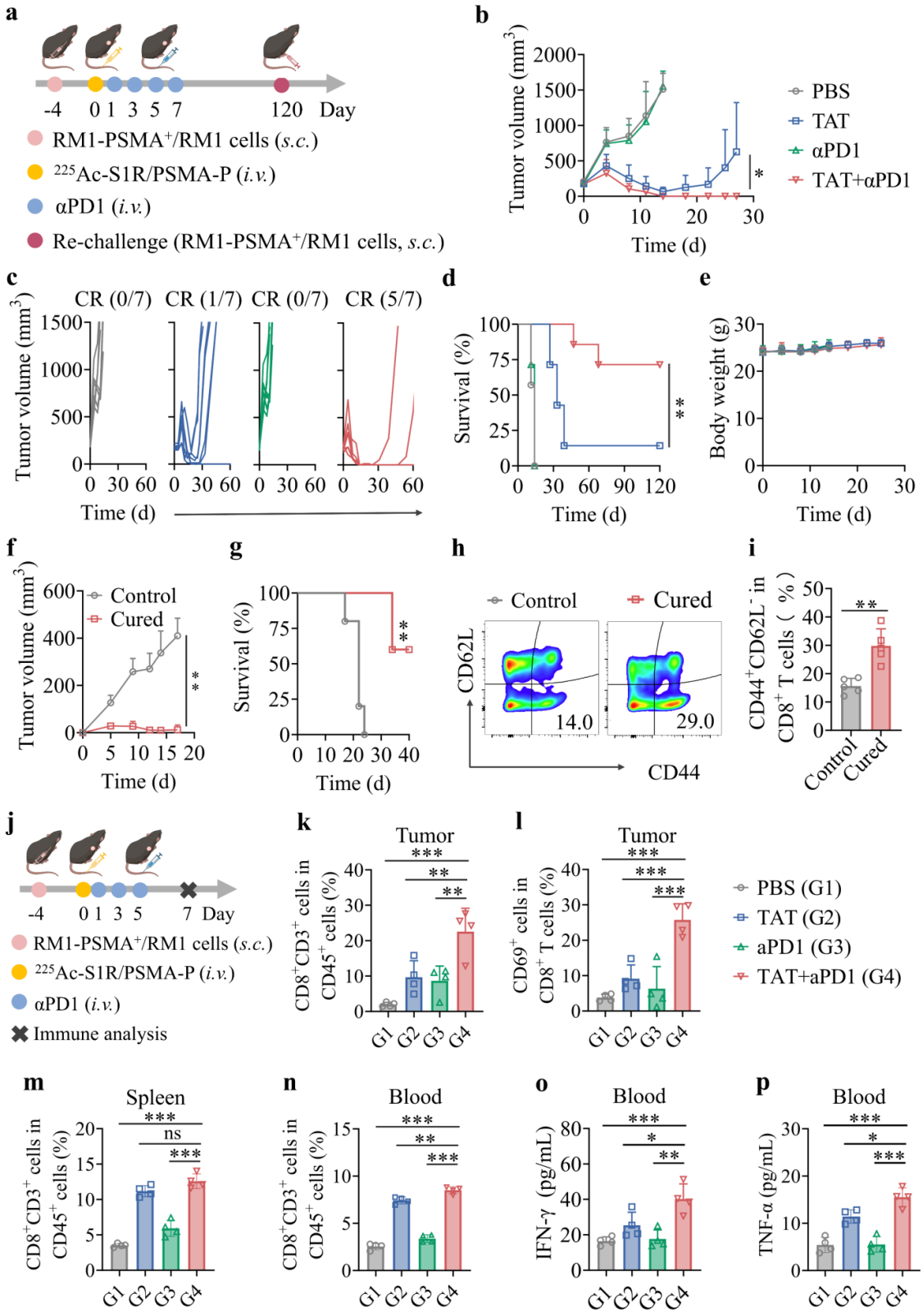

Fig. 5 ^{225}Ac-S1R/PSMA-P boosts immune checkpoint blockade therapy in RM1-PSMA^{+}/RM1 tumor-bearing mice. TAT refers to ^{225}Ac-S1R/PSMA-P at 3.7 kBq, and αPD1 represents *i.v.* injection of αPD1 antibody at a dose of 10 μg. (a) Experimental schedule for figures b-i. (b) Tumor growth curves, (c) individual tumor growth curves, (d)

Kaplan-Meier survival curves, and (e) average body weights of the mice treated with PBS, TAT, αPD1, or TAT+αPD1. (f) Tumor growth curves and (g) Kaplan-Meier survival curves of mice re-challenged at 120 days after ^{225}Ac-S1R/PSMA-P treatment. (h) Representative flow cytometry graphs and (i) percentages of effector memory T cells (T_{em}, $CD8^+CD44^+CD62L^-$) in $CD8^+$ T cells in peripheral blood following re-challenge. (j) Experimental workflow of immunotherapy and analysis of immune responses for figures k-p. (k) $CD3^+CD8^+$ T cells in $CD45^+$ cells and (l) $CD69^+$ in $CD8^+$ T cells within tumor. Contents of $CD8^+$ T cells in the (m) spleen and (n) peripheral blood. Expression levels of (o) IFN-γ and (p) TNF-α in serum analyzed by ELISA. Statistical significance was analyzed by one-way ANOVA, * $p < 0.1$, ** $p < 0.01$, and *** $p < 0.001$.

We further investigated the immunological responses (immune cells and cytokines) of the mice following combo therapy. The results showed that 3.7 kBq of ^{225}Ac-S1R/PSMA-P combined with αPD1 significantly increased the percentage of $CD8^+$ tumor-infiltrating T lymphocytes ($CD45^+CD3^+CD8^+$) in the tumor (**Fig. 5k**). We further found an increase of activated CD8 T cells ($CD8^+CD69^+$) in the tumor (**Fig. 5l**), indicating cytotoxic T cells are activated at an early stage. The combo therapy also led to a higher ratio of $CD8^+$ T cells within the spleen and blood (**Figs. 5m and 5n**) and an increase in serum IFN-γ cytokine and TNF-α secretion (**Figs. 5o and 5p**). These results confirm that ^{225}Ac-S1R/PSMA-P in combination with αPD-1 elicits robust and durable anti-tumor immune responses.

ICB is one of the most exciting developments in clinical cancer treatment; however, a majority of patients do not respond to ICB therapy [57]. TRT has appeared to be an effective strategy to enhance the response rate of ICB [58-62]. Furthermore, in an open-label phase 1 clinical trial, a single dose of ^{177}Lu-PSMA-617 followed by pembrolizumab treatment brought about durable clinical benefit in mCRPC patients [63]. The results of this study show that a very low dose of ^{225}Ac-S1R/PSMA-P can convert immunologically "cold" prostate tumor into "hot" and markedly boost αPD1 therapy, achieving CR in 5 out of 7 RM1-$PSMA^+$/RM1 tumor-bearing mice. The low dose of ^{225}Ac-S1R/PSMA-P is beneficial, as it will not only

greatly reduce treatment cost but also improve safety and minimize damage to immune system. PSMA is also overexpressed in the neovasculature of several malignant tumors such as lung, breast, and gastric cancers [64-66], which renders ^{225}Ac-S1R/PSMA-P potentially interesting for boosting ICB therapy across various tumor types.

4. Conclusion

We have demonstrated that Sigma-1 receptor and PSMA dual-specific radioligand (S1R/PSMA-P) mediates superior alpha therapy and alpha-immunotherapy of malignant prostate tumor. Of note, ^{225}Ac-S1R/PSMA-P showed an extraordinary tumor selectivity, uptake and retention, which could effectively shrink large PSMA-positive LNCaP-FGC tumor at 1.85 kBq and completely regress highly malignant murine RM1-PSMA^{+}/RM1 tumor at 33.3 kBq. More interestingly, a low dose of ^{225}Ac-S1R/PSMA-P could induce ICD of tumor cells and reverse the suppressive tumor microenvironment, and boost immune checkpoint blockade therapy with αPD1, leading to 5/7 of the mice free of tumor. The cured mice exhibit long anti-cancer immune memory effect. These findings highlight the significant clinical potential of ^{225}Ac-S1R/PSMA-P as a novel therapeutic radiopharmaceutical for the treatment of advanced prostate cancer.

CRediT authorship contribution statement

Juan Sun: Writing-original draft, Investigation, Formal analysis, Data curation, Conceptualization. **Jiangtao Yang:** Validation, Project administration, Investigation, Formal analysis, Data curation. **JiaKun Guo:** Writing-original draft, Methodology, Investigation, Formal analysis, Data curation. **Lei Tao:** Methodology, Investigation, Formal analysis, Data curation. **Bin Xu:** Methodology, Investigation, Formal analysis, Data curation. **Guanglin Wang:** Writing-review & editing, Validation, Supervision, Resources, Data curation,

Conceptualization. **Fenghua Meng:** Supervision, Resources, Project administration, Investigation. **Zhiyuan Zhong:** Writing review & editing, Writing-original draft, Supervision, Funding acquisition, Conceptualization

Notes

The authors declare no competing financial interest.

Acknowledgements

This work is supported by research grants from the National Natural Science Foundation of China (52233007), and the Project of State Key Laboratory of Radiation Medicine and Protection (GZC00401).

References

[1] M. Senior, Precision radiation opens a new window on cancer therapy, Nat Biotechnol. 42 (2024) 1003-1008.

[2] L. Bodei, K. Herrmann, H. Schöder, et al., Radiotheranostics in oncology: current challenges and emerging opportunities, Nat Rev Clin Oncol. 19 (2022) 534-550.

[3] E.O. Aboagye, T.D. Barwick, U. Haberkorn, Radiotheranostics in oncology: Making precision medicine possible, CA Cancer J Clin. 73 (2023) 255-274.

[4] J. Sun, Z. Huangfu, J. Yang, et al., Imaging-Guided Targeted Radionuclide Tumor Therapy: From Concept to Clinical Translation, Adv Drug Deliv Rev. (2022) 114538-114561.

[5] D.A. Jaffray, F. Knaul, M. Baumann, et al., Harnessing progress in radiotherapy for global cancer control, Nat Cancer. 4 (2023) 1228-1238.

[6] N.L. Albert, E. Le Rhun, G. Minniti, et al., Translating the theranostic concept to neuro-oncology: disrupting barriers, Lancet Oncol. 25 (2024) 441-451.

[7] K.L. Pomykala, B.A. Hadaschik, O. Sartor, et al., Next generation radiotheranostics promoting precision medicine, Ann Oncol. 34 (2023) 507-519.

[8] M.B. Sonbol, T.R. Halfdanarson, T. Hilal, Assessment of Therapy-Related Myeloid Neoplasms in Patients With Neuroendocrine Tumors After Peptide Receptor Radionuclide Therapy: A Systematic Review, JAMA Oncol. 6 (2020) 1086-1092.

[9] A.S. Parihar, M.S. Hofman, A. Iravani, 177Lu–Prostate-specific Membrane Antigen Radioligand Therapy in Patients with Metastatic Castration-resistant Prostate Cancer, Radiology. 306 (2022) 220859-220867.

[10] N. Alan-Selcuk, G. Beydagi, E. Demirci, et al., Clinical Experience with 225Ac Ac-PSMA Treatment in Patients with 177Lu Lu-PSMA-Refractory Metastatic Castration-Resistant Prostate Cancer, J Nucl Med. 64 (2023) 1574-1580.

[11] A. Gaeble, A. Dierks, A. Rinscheid, et al., Experience of rescue therapy with177Lu-rhPSMA-10.1 in patients with primary or acquired resistance to 177Lu-PSMA-I&T, Eur J Nucl Med Mol Imaging. (2024) 9.

[12] J. Strosberg, G. El-Haddad, E. Wolin, et al., Phase 3 Trial of 177Lu-Dotatate for Midgut Neuroendocrine Tumors, N Engl J Med. 376 (2017) 125-135.

[13] B. Feuerecker, R. Tauber, K. Knorr, et al., Activity and Adverse Events of Actinium-225-PSMA-617 in Advanced Metastatic Castration-resistant Prostate Cancer After Failure of Lutetium-177-PSMA, Eur Urol. 79 (2021) 343-350.

[14] G. De Vincentis, W. Gerritsen, J.E. Gschwend, et al., Advances in targeted alpha therapy for prostate cancer, Ann Oncol. 30 (2019) 1728-1739.

[15] Z. Huangfu, J. Yang, J. Sun, et al., PSMA and Sigma-1 receptor dual-targeted peptide mediates superior radionuclide imaging and therapy of prostate cancer, J Control Release. 375 (2024) 767-775.

[16] M. Sathekge, A. Morgenstern, Advances in targeted alpha therapy of cancer, Eur J Nucl Med Mol Imaging. 51 (2024) 1205-1206.

[17] M.R. McDevitt, D. Ma, L.T. Lai, et al., Tumor Therapy with Targeted Atomic Nanogenerators, Science. 294 (2001) 1537-1540.

[18] J. Ding, S.S. Qin, X.G. Hou, et al., Recent advances in emerging radiopharmaceuticals and the challenges in radiochemistry and analytical chemistry, Trends Analyt Chem. 182 (2025) 118053-118073.

[19] E.A.M. Ruigrok, G. Tamborino, E. de Blois, et al., In vitro dose effect relationships of

actinium-225-and lutetium-177-labeled PSMA-I&T, Eur J Nucl Med Mol Imaging. 49 (2022) 3627-3638.

[20] Y.-H. Dai, P.-H. Chen, D.-J. Lee, et al., A Meta-Analysis and Meta-Regression of the Efficacy, Toxicity, and Quality of Life Outcomes Following Prostate-Specific Membrane Antigen Radioligand Therapy Utilising Lutetium-177 and Actinium-225 in Metastatic Prostate Cancer, Eur Urol. (2024).

[21] J.M. Pagel, A.L. Kenoyer, T. Bäck, et al., Anti-CD45 pretargeted radioimmunotherapy using bismuth-213: high rates of complete remission and long-term survival in a mouse myeloid leukemia xenograft model, Blood. 118 (2011) 703-711.

[22] K.A. Morgan, S.E. Rudd, A. Noor, et al., Theranostic Nuclear Medicine with Gallium-68, Lutetium-177, Copper-64/67, Actinium-225, and Lead-212/203 Radionuclides, Chem Rev. 123 (2023) 12004-12035.

[23] M.M. Sathekge, I.O. Lawal, C. Bal, et al., Actinium-225-PSMA radioligand therapy of metastatic castration-resistant prostate cancer (WARMTH Act): a multicentre, retrospective study, Lancet Oncol. 25 (2024) 175-183.

[24] D. Ludwig, R. Bryan, W. Dawicki, et al., Preclinical Development of an Actinium-225-Labeled Antibody Radio-Conjugate Directed Against CD45 for Targeted Conditioning and Radioimmunotherapy, Blood. 134 (2019) 5601-5603.

[25] G.A. Ulaner, L.A. VanderMolen, G. Li, et al., Dotatate PET/CT and 225Ac-Dotatate Therapy for Somatostatin Receptor–expressing Metastatic Breast Cancer, Radiology. 312 (2024) 233408-233415.

[26] A. Morgenstern, C. Apostolidis, F. Bruchertseifer, Supply and Clinical Application of Actinium-225 and Bismuth-213, Semin Nucl Med 50 (2020) 119-123.

[27] L. Chen, Y.-X. Xu, Y.-S. Wang, et al., Prostate cancer microenvironment: multidimensional regulation of immune cells, vascular system, stromal cells, and microbiota, Mol Cancer. 23 (2024) 229-260.

[28] A. Lyu, Z.H. Fan, M. Clark, et al., Evolution of myeloid-mediated immunotherapy resistance in prostate cancer, Nature (2024) 35.

[29] E.S. Antonarakis, J.M. Piulats, M. Gross-Goupil, et al., Pembrolizumab for Treatment-Refractory Metastatic Castration-Resistant Prostate Cancer: Multicohort,

Open-Label Phase II KEYNOTE-199 Study, J Clin Oncol. 38 (2020) 395-405.

[30] R.C. Winter, M. Amghar, A.S. Wacker, et al., Future Treatment Strategies for Cancer Patients Combining Targeted Alpha Therapy with Pillars of Cancer Treatment: External Beam Radiation Therapy, Checkpoint Inhibition Immunotherapy, Cytostatic Chemotherapy, and Brachytherapy, Pharmaceuticals (Basel). 17 (2024) 1031-1077.

[31] S. Lunj, T.A.D. Smith, K.J. Reeves, et al., Immune effects of α and β radionuclides in metastatic prostate cancer, Nat Rev Urol. 21 (2024) 651-661.

[32] J. Zhang, F. Li, Y. Yin, et al., Alpha radionuclide-chelated radioimmunotherapy promoters enable local radiotherapy/chemodynamic therapy to discourage cancer progression, Biomater Res. 26 (2022) 44-58.

[33] S.D. Mare, Y. Nishri, A. Shai, et al., Diffusing Alpha-Emitters Radiation Therapy Promotes a Proimmunogenic Tumor Microenvironment and Synergizes With Programmed Cell Death Protein 1 Blockade, Int J Radiat Oncol Biol Phys. 115 (2023) 707-718.

[34] J. Zhang, S. Zhang, C. Cheng, et al., Targeting senescence with radioactive 223Ra/Ba SAzymes enables senolytics-unlocked One‐Two punch strategy to boost anti-tumor immunotherapy, Biomaterials. 315 (2025) 122915-122928.

[35] M. Li, D. Liu, D. Lee, et al., Targeted Alpha-Particle Radiotherapy and Immune Checkpoint Inhibitors Induces Cooperative Inhibition on Tumor Growth of Malignant Melanoma, Cancers (Basel). 13 (2021) 3676-3693.

[36] M.J. Zacherl, F.J. Gildehaus, L. Mittlmeier, et al., First Clinical Results for PSMA-Targeted α-Therapy Using 225Ac-PSMA-I&T in Advanced-mCRPC Patients, J Nucl Med. 62 (2021) 669-674.

[37] W.P. Fendler, A.D. Stuparu, S. Evans-Axelsson, et al., Establishing (177)Lu-PSMA-617 Radioligand Therapy in a Syngeneic Model of Murine Prostate Cancer, J Nucl Med. 58 (2017) 1786-1792.

[38] S. Poty, L.M. Carter, K. Mandleywala, et al., Leveraging Bioorthogonal Click Chemistry to Improve (225)Ac-Radioimmunotherapy of Pancreatic Ductal Adenocarcinoma, Clin Cancer Res. 25 (2019) 868-880.

[39] K. Jewell, M.S. Hofman, J.S.L. Ong, et al., Emerging Theranostics for Prostate Cancer and a Model of Prostate-specific Membrane Antigen Therapy, Radiology. 311 (2024)

231703-231712.

[40] A. van Waarde, A.A. Rybczynska, N.K. Ramakrishnan, et al., Potential applications for sigma receptor ligands in cancer diagnosis and therapy, Biochim Biophys Acta. 1848 (2015) 2703-2716.

[41] E. Aydar, P. Onganer, R. Perrett, et al., The expression and functional characterization of sigma (sigma) 1 receptors in breast cancer cell lines, Cancer Lett 242 (2006) 245-257.

[42] B.J. Vilner, C.S. John, W.D. Bowen, Sigma-1 and sigma-2 receptors are expressed in a wide variety of human and rodent tumor cell lines, Cancer Res 55 (1995) 408-420.

[43] M.R. McDevitt, D. Ma, L.T. Lai, et al., Tumor Therapy with Targeted Atomic Nanogenerators, Science. 294 (2001) 1537-1540.

[44] M. Perera, N. Papa, D. Christidis, et al., Sensitivity, Specificity, and Predictors of Positive (68)Ga-Prostate-specific Membrane Antigen Positron Emission Tomography in Advanced Prostate Cancer: A Systematic Review and Meta-analysis, Eur Urol. 70 (2016) 926-937.

[45] K.A. Deal, I.A. Davis, S. Mirzadeh, et al., Improved in vivo stability of actinium-225 macrocyclic complexes, J Med Chem. 42 (1999) 2988-2992.

[46] G. Wang, R.M. de Kruijff, A. Rol, et al., Retention studies of recoiling daughter nuclides of 225Ac in polymer vesicles, Appl Radiat Isot. 85 (2014) 45-53.

[47] G.J.P. Deblonde, M. Zavarin, A.B. Kersting, The coordination properties and ionic radius of actinium: A 120-year-old enigma, Coord Chem Rev. 446 (2021) 214130-214150.

[48] J.B. Gorin, Y. Guilloux, A. Morgenstern, et al., Using α radiation to boost cancer immunity?, Oncoimmunology. 3 (2014) 954925-954926.

[49] S. Lunj, T.A.D. Smith, K.J. Reeves, et al., Immune effects of α and β radionuclides in metastatic prostate cancer, Nat Rev Urol. 21 (2024) 651-661.

[50] Z. Cui, L. Wang, W. Liu, et al., Imageable Brachytherapy with Chelator-Free Radiolabeling Hydrogel, Adv Healthc Mater. 13 (2024) 2401438-2401447.

[51] M. Yang, H. Liu, J. Lou, et al., Alpha-Emitter Radium-223 Induces STING-Dependent Pyroptosis to Trigger Robust Antitumor Immunity, Small. 20 (2024) 2307448-2307462.

[52] S. Qin, Y. Yang, J. Zhang, et al., Effective Treatment of SSTR2-Positive Small Cell Lung Cancer Using 211At-Containing Targeted α-Particle Therapy Agent Which Promotes

Endogenous Antitumor Immune Response, Mol Pharm. 20 (2023) 5543-5553.

[53] J.B. Gorin, J. Ménager, S. Gouard, et al., Antitumor immunity induced after α irradiation, Neoplasia. 16 (2014) 319-328.

[54] J. Czernin, K. Current, C.E. Mona, et al., Immune-Checkpoint Blockade Enhances (225)Ac-PSMA617 Efficacy in a Mouse Model of Prostate Cancer, J Nucl Med. 62 (2021) 228-231.

[55] H. Dabagian, T. Taghvaee, P. Martorano, et al., PARP Targeted Alpha-Particle Therapy Enhances Response to PD-1 Immune-Checkpoint Blockade in a Syngeneic Mouse Model of Glioblastoma, ACS Pharmacol Transl Sci. 4 (2021) 344-351.

[56] S.-L. Cheng, H.-M. Lee, C.-P. Li, et al., Robust and Sustained STING Pathway Activation via Hydrogel-Based In Situ Vaccination for Cancer Immunotherapy, ACS Nano. 18 (2024) 29439-29456.

[57] B. Wu, B. Zhang, B.W. Li, et al., Cold and hot tumors: from molecular mechanisms to targeted therapy, Signal Transduct Target Ther. 9 (2024) 65.

[58] J. Chen, Y. Zhou, Y. Pang, et al., FAP-targeted radioligand therapy with (68)Ga/(177)Lu-DOTA-2P(FAPI)(2) enhance immunogenicity and synergize with PD-L1 inhibitors for improved antitumor efficacy, J Immunother Cancer 13 (2025).

[59] R.B. Patel, R. Hernandez, P. Carlson, et al., Low-dose targeted radionuclide therapy renders immunologically cold tumors responsive to immune checkpoint blockade, Sci Transl Med 13 (2021) 17.

[60] H.J. Chen, L. Zhao, K.L. Fu, et al., Integrin αvβ3-targeted radionuclide therapy combined with immune checkpoint blockade immunotherapy synergistically enhances anti-tumor efficacy, Theranostics. 9 (2019) 7948-7960.

[61] J. Choi, W. Beaino, R.J. Fecek, et al., Combined VLA-4-Targeted Radionuclide Therapy and Immunotherapy in a Mouse Model of Melanoma, J Nucl Med. 59 (2018) 1843-1849.

[62] L. Zhao, Y. Pang, Y. Zhou, et al., Antitumor efficacy and potential mechanism of FAP-targeted radioligand therapy combined with immune checkpoint blockade, Signal Transduct Target Ther. 9 (2024) 142.

[63] R. Aggarwal, S. Starzinski, I. de Kouchkovsky, et al., Single-dose 177Lu-PSMA-617 followed by maintenance pembrolizumab in patients with metastatic castration-resistant

prostate cancer: an open-label, dose-expansion, phase 1 trial, Lancet Oncol. 24 (2023) 1266-1276.

[64] M. Kasoha, C. Unger, E.F. Solomayer, et al., Prostate-specific membrane antigen (PSMA) expression in breast cancer and its metastases, Clin Exp Metastasis. 34 (2017) 479-490.

[65] L.X. Chen, S.J. Zou, D. Li, et al., Prostate-specific membrane antigen expression in hepatocellular carcinoma, cholangiocarcinoma, and liver cirrhosis, World J Gastroenterol. 26 (2020) 7664-7678.

[66] M.J.M. Uijen, Y.H.W. Derks, R.I.J. Merkx, et al., PSMA radioligand therapy for solid tumors other than prostate cancer: background, opportunities, challenges, and first clinical reports, Eur J Nucl Med Mol Imaging. 48 (2021) 4350-4368.

Graphical Abstract

`

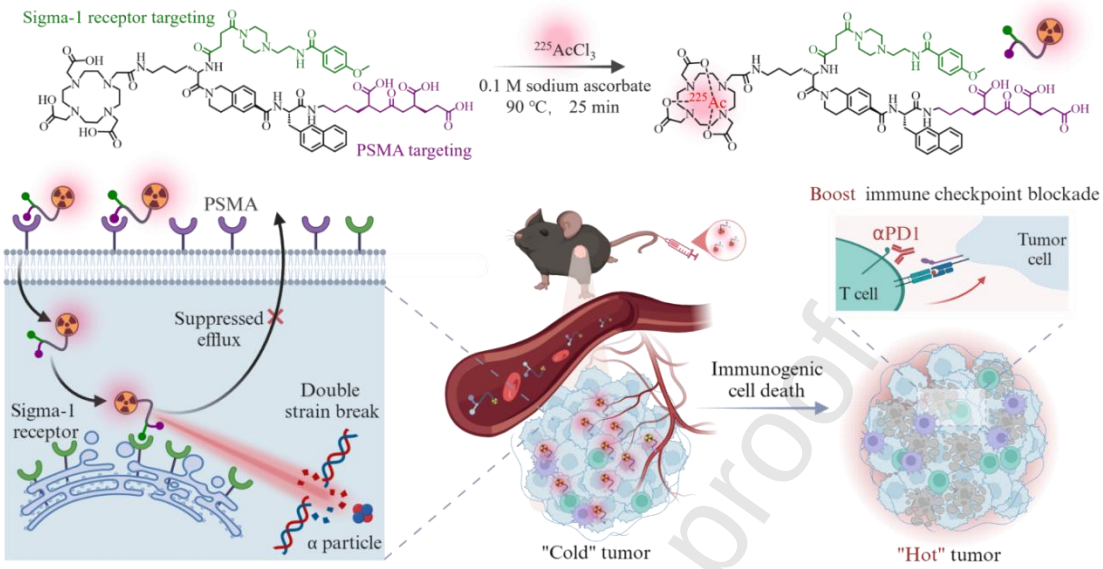

Sigma-1 receptor and PSMA dual-specific radioligand (S1R/PSMA-P) induces high-efficacy alpha therapy and immunotherapy, leading to complete regression of highly malignant murine prostate tumor.

Highlights

1. Sigma-1 receptor and PSMA dual-specific peptide (S1R/PSMA-P) boosts cell uptake and retention of ^{225}Ac by inhibiting drug efflux.
2. ^{225}Ac-S1R/PSMA-P exhibits high uptake and long retention in the PSMA-positive prostate tumor.
3. A single low dose of ^{225}Ac-S1R/PSMA-P (1.85 kBq) effectively shrinks large PSMA-positive LNCaP-FGC tumor xenografts.
4. A low dose of ^{225}Ac-S1R/PSMA-P (3.7 kBq) boosts αPD1 therapy of "cold" murine prostate tumor.